

# Obfuscated Location Disclosure for Remote ID Enabled Drones

Alessandro Brighente, Mauro Conti, Matthijs Schotsman, Savio Sciancalepore



arXiv:2407.14256v1 [cs.CR] 19 Jul 2024

**Abstract**—The Remote ID (RID) regulation recently introduced by several aviation authorities worldwide (including the US and EU) forces commercial drones to regularly (max. every second) broadcast plain-text messages on the wireless channel, providing information about the drone identifier and current location, among others. Although these regulations increase the accountability of drone operations and improve traffic management, they allow malicious users to track drones via the disclosed information, possibly leading to drone capture and severe privacy leaks.

In this paper, we propose Obfuscated Location disclosure for RID-enabled drones (OLO-RID), a solution modifying and extending the RID regulation while preserving drones' location privacy. Rather than disclosing the actual drone's location, drones equipped with OLO-RID disclose a differentially private obfuscated location in a mobile scenario. OLO-RID also extends RID messages with encrypted location information, accessible only by authorized entities and valuable to obtain the current drone's location in safety-critical use cases. We design, implement, and deploy OLO-RID on a Raspberry Pi 3 and release the code of our implementation as open-source. We also perform an extensive performance assessment of the runtime overhead of our solution in terms of processing, communication, memory, and energy consumption. We show that OLO-RID can generate RID messages on a constrained device in less than 0.16 s while also requiring a minimal energy toll on a relevant device (0.0236% of energy for a DJI Mini 2). We also evaluate the utility of the proposed approach in the context of three reference use cases involving the drones' location usage, demonstrating minimal performance degradation when trading off location privacy and utility for next-generation RID-compliant drone ecosystems.

## 1 INTRODUCTION

The adoption of Unmanned Aerial Vehicles (UAVs), a.k.a. drones, is increasing today in many application areas, e.g., search-and-rescue, surveillance, goods delivery, and agriculture [1]. Such pervasive diffusion is also supported by reports of leading market companies, forecasting over 9.6 million consumer drone unit shipments globally by 2030, with 865 million devices already deployed in 2023 [2], [3].

At the same time, relevant regional aviation authorities need to integrate drones into the local airspaces to enhance

monitoring and accountability of drone operations. To this aim, many aviation authorities, e.g., the US-based Federal Aviation Administration (FAA) and the EU-based European Union Aviation Safety Agency (EASA), mandated remote identification of drones through dedicated Remote ID (RID) rules [4], [5]. According to such regulations, drones should constantly broadcast on the wireless channel RID messages containing a unique identifier, the drone's current location (latitude, longitude, altitude) and velocity, the location of the corresponding Control Station (CS), a time mark, and an emergency status indication. RID messages should be emitted no less than once a second in plain text, using either WiFi or BLE—when such communication technologies are unavailable onboard, the drone should be equipped with dedicated external RID modules.

Despite solving drones' accountability issues, RID regulations introduce confidentiality and privacy issues. Adversaries can track drones using a (network of) passive receiver(s). In turn, such tracking can lead to the leakage of private information about the drone, its pilot, and the drone-based business. For instance, the source location can be traced back to the location of warehouses, the flight destination can lead to customers' private location disclosure, and the track can reveal IP-protected information about the algorithm used for navigation [6]. A few works investigated privacy issues connected with RID, mainly considering the identity of the drone and collision avoidance strategies [6], [7]. However, to preserve full compliance with RID regulations, at the time of this writing, no works considered drone's location privacy. The mentioned problem shares similarities with privacy issues affecting users interacting with Location-Based Services (LBSs), where users would like to get suggestions based on their current location while not allowing LBSs providers to track them. However, providing location privacy to RID-enabled drones further complicates the problem, due to the required frequent information broadcast that makes the disclosed locations highly correlated in time and space. Moreover, compared to users' devices (smartphones and laptops), drones may not be persistently connected to the Internet. Also, drones can be much more constrained in terms of processing, memory, communication, and energy availability, calling for very lightweight approaches. Overall, although we know from the literature that any location obfuscation mechanism is bound to cause privacy loss when used repeatedly [8], a solution specifically tailored to the use cases of RID-enabled

- Alessandro Brighente and Mauro Conti are with the University of Padova, Department of Information Engineering, Italy. e-mails: {alessandro.brighente, mauro.conti}@unipd.it.
  - Matthijs Schotsman and Savio Sciancalepore are with the Eindhoven University of Technology (TU/e), Department of Mathematics and Computer Science, Eindhoven, The Netherlands. e-mails: m.schotsman@student.tue.nl, s.sciancalepore@tue.nl.
- Alphabetical order of the authors.

drones is currently not available.

**Contribution.** In our work, we design Obfuscated Location disclosure for RID-enabled drones (OLO-RID), a framework that allows RID-compliant drones to protect as much as possible their current location while allowing relevant location-based services (using such location) to keep working reliably and efficiently. Our solution integrates and extends the mechanism proposed by Xiao et al. in [9], making it suitable to run at runtime on drones while fulfilling all the requirements imposed by RID. We also extend the RID regulation through encrypted location reports that relevant authorities can use to disclose the drone location if necessary. We implement our proposed solution on two Proof-of-Concepts (PoCs) devices, using a general-purpose laptop and a constrained embedded system Raspberry PI 3 Model B+ (RPI), featuring similar hardware constraints to medium-end drones, and release the code of our implementation as open-source [10]. Through an extensive experimental measurement campaign, we show that OLO-RID can run on relevant platforms by requiring less than 0.16 s and 0.0236% of energy—considering the energy available on a DJI Mini 2. We also introduce three among the most relevant real-world use cases involving the usage of the drones’ location and extract utility metrics to determine the impact of the disclosure of an obfuscated location on the quality of the services offered. Overall, we evaluate the trade-off between drones’ location privacy and utility, showing the possibility of letting the two requirements coexist meaningfully and effectively.

Note that this work extends and completes our preliminary study in [11] through the following contributions.

- We replace the basic Geo-Indistinguishability method used in [11] with a solution inspired by the proposal by Xiao et al. in [9], specifically conceived for time-correlated location disclosures, modified on purpose to fit the scenario of RID-enabled drones.
- We implement the proposed solution on two PoC platforms and release the code as open-source [10].
- We evaluate the overhead of our solution on real drones’ trajectory data in terms of execution time, memory, bandwidth, and energy consumption.
- We apply our solution to three relevant real-world use cases in the content of drone-based location-based services. We then show the trade-off existing between location privacy and utility in our proposed solution.

**Roadmap.** This paper is organized as follows. Sec. 2 introduces the preliminaries; Sec. 3 describes the scenario, adversarial model, use cases, and requirements; Sec. 4 discusses related work and evaluates their match to our requirements; Sec. 5 introduces OLO-RID; Sec. 6 provides security considerations; Sec. 7 introduces our PoC; Sec. 8 discusses our extensive performance assessment; Sec. 9 discusses the results; and finally, Sec. 10 concludes the paper.

## 2 PRELIMINARIES

### 2.1 Remote ID

Remote ID (RID) is a standard regulation first published in 2021 by the FAA [4], whose goal is to enhance the

accountability of UAV operations and use the airspace efficiently while prioritizing public safety. This regulation forces almost all UAVs to emit wireless messages at least once each second, reporting the drone’s unique identity and location, the pilot’s (CS) location, the timestamp and emergency status. The regulation defines two RID modes, i.e., Network RID and Broadcast RID. In Network RID, the UAV delivers unicast RID messages to a third-party service provider over the Internet, possibly relaying such messages through the CS. In Broadcast RID, the UAV broadcasts RID messages using Wi-Fi or Bluetooth so that any compatible receiver nearby can receive such information. Drones not equipped with a compatible transceiver must integrate external RID modules provided by relevant companies. This manuscript focuses explicitly on the Broadcast RID mode, as this scenario presents unique challenges in realistic operational conditions. The RID rule applies to drones weighing more than 250 g anywhere except FAA-Recognized Identification Areas, explicitly listed in the regulation. RID does not specify any security measures applying to the delivered messages, leaving them free to the implementation. Thus, by default, RID messages are delivered in plaintext. Also, the RID regulation does not provide specific techniques for deploying RID in real-world scenarios. The Drone Remote ID Protocol (DRIP) Working Group (WG) of the IETF takes such gaps into account and is currently working on deployment and security requirements connected to RID [12]. Throughout several documents and Request for Comments (RFCs), the WG defines the network architecture for RID-compliance deployments, requirements and necessary protocols [13], [14]. In this work, we align the network architecture, the names of the entities, and the design requirements to the ones defined by DRIP to create a standard-compliant solution and smooth the possible integration of our solution into standardization activities.

### 2.2 Public Key Encryption

Public Key Encryption (Public Key Encryption (PKE)) techniques allow encrypting a plaintext message  $m$  using the public key of the recipient  $pk_R$  to a ciphertext  $c$ , such that the recipient, in possession of the corresponding private key  $sk_R$ , is the only party able to decrypt the ciphertext and obtain the plaintext.

**Definition 1.** A public key encryption algorithm  $PKE$  includes the following algorithms:

$PKE.KGen(1^k)$ : on input a security parameter  $k$ , it outputs a secret decryption key  $sk$  and a public encryption key  $pk$ .

$PKE.Enc(pk_R, m)$ : on input a plaintext message  $m$  and a public key  $pk_R$ , it outputs a ciphertext  $c$ .

$PKE.Dec(sk_R, c)$ : on input a ciphertext  $c$  and a private decryption key  $sk_R$ , it outputs the corresponding plaintext  $m$ .

In this manuscript, we use the well-known Elliptic Curve Integrated Encryption Scheme (ECIES) as a PKE technique [15].

### 3 SCENARIO, USE CASES, AND REQUIREMENTS

#### 3.1 Scenario and assumptions

We consider a UAV compliant with the RID regulation. Thus, it integrates a *RID Module* that wirelessly broadcasts RID messages from takeoff to shutdown. As discussed in Sec. 2.1, RID messages contain a unique identifier of the UAV  $UID$ , the UAV's location data (latitude, longitude, and altitude)  $\mathbf{z}$ , the UAV's current velocity  $\mathbf{v}$ , the CS's current location (latitude, longitude, and altitude)  $\mathbf{x}_{CS}$ , a timestamp  $t$ , and the emergency status indication  $em_t$ . As per the regulation, we consider that the UAV has to broadcast a RID message at least once a second, reporting every time an updated location. We consider drones broadcasting RID messages via WiFi, so as to maximize transmission range while keeping compliance with the RID rule. Consider that WiFi transceivers installed on drones can reach extensive ranges, up to 7 km, guaranteeing sufficient coverage [16]. We consider UAVs carrying a *Global Navigation Satellite System (GNSS) Module* to obtain the current location  $\mathbf{x}$ , e.g., a Global Positioning System (GPS) receiver. Moreover, we consider UAVs with enough computational power and energy to run basic cryptography algorithms, such as a PKE scheme, through an *Encryption Module*. Based on the considered use case (see Sec. 3.3), the drone might operate in scenarios with an intermittent or unavailable Internet connection. Therefore, our solution (see Sec. 5) does not require the existence of a persistent connection of the drone to any Cloud Service Provider (CSP). Although some use cases discussed below might describe the connection of drones to external services, such connection is never required to execute our solution. We also envision the presence of a dedicated process, namely the *Obfuscation Module*, aimed at generating an obfuscated location according to our solution. Onboard the drone, for some use cases, we also consider the presence of a *Communication Module*, aimed at establishing mutual communication with other entities. This module can be installed by the owner of the drone, based on the envisioned use case. We do not make any assumption about the operational mode of the UAV, which can be either remotely piloted or autonomous. However, as for the CS location, we consider it is either already stored on the UAV or updated thanks to real-time communication with the CS. We also consider one or more wireless receivers, which we refer to as *observers*, in line with the standard DRIP architecture. Observers are entities that can receive RID messages on a compatible RF interface. As defined in RFC 9153 [13], we consider multiple types of observers, namely General Public Observers, and Public Safety Observers. Public Safety Observers are part of a more extensive sensing infrastructure focusing on public safety and security. General Public Observers can be regular users receiving RID messages without relationships with specific sensing infrastructures. Our system model also includes a Trusted Third Party (TTP), responsible for storing identifiers and cryptographic materials used to secure RID messages. As per the architecture defined by DRIP, we refer to the TTP as the Unmanned Service Supplier (USS). Storage and retrieval of information from the USS can be done through dedicated registries. In line with DRIP, we distinguish between public and private registries [12]. Using the drones' unique identifier, anyone

can use the public registry to retrieve public information. Conversely, only authorized parties can use the private registry to retrieve confidential data. The TTP is always available online, so parties can interact with it if required.

In our work, we want to design a location obfuscation mechanism to protect drones' actual location when disclosing RID messages, despite the presence of time correlation in the disclosed locations. In Sec. 3.3, we provide a few use cases relevant to our investigation. We report the main notation used in the manuscript in the Appendix (supplementary materials).

#### 3.2 Adversary Model

The adversary considered in this work is a passive eavesdropper, namely  $\epsilon$ , who aims to track the UAV based on the disclosed RID messages. As drones deliver RID messages in plaintext,  $\epsilon$  can achieve this aim by simply using a receiver compatible with the communication technology (WiFi). Using the retrieved location information, the attacker can track the UAV and deduct private information about the business the drone is used for and the pilot. Such information can be further exploited to take a UAV down, capture it and steal any carried goods or private data stored onboard. All such actions could damage the UAV, the business using the drones, and potentially the safety of the people involved. In line with relevant literature [6] [17], our work considers honest UAVs. We intentionally do not consider scenarios where the pilot purposely turns off RID or tamper with the RID module to carry out unauthorized actions, as this would involve malicious UAVs, which are not in the scope of our paper nor the RID regulation. On the contrary, our work intends to protect the privacy of RID-compliant drones and the business using the drone from tracking and other threats, to finally unleash the potential behind drone usage in various application domains.

#### 3.3 Use Cases

In the following, we describe three real-world use cases motivating the deployment of our solution.

**Use Case 1: Unintentional Invasion of No-Fly Zone.** We consider a legitimate UAV operating near an No-Fly Zone (NFZ). An NFZ is an area where UAVs are not allowed to fly, e.g., around Critical Infrastructures (CIs) such as airports and power distribution grids. We consider that the CI operator maintaining the site deploys one or more observers to monitor the area of the NFZ for drone invasions (among other factors)—based on DRIP, such observers are *public safety observers*. Based on the deployed observers' area coverage, the system's overall reception range could extend outside the boundaries of the NFZ. We define the portion of the coverage area outside of the NFZ as the Warning Area (WA). In principle, UAVs are allowed to fly in the WA. When receiving RID messages, the observers use the disclosed location to check if the drone is invading the NFZ. If this is the case, they take action and use the disclosed location to take the drone down (e.g., by jamming or physically shutting it down—through weapons or nets) [18]. Consider

drones disclosing an obfuscated location through RID messages rather than the actual one, and approaching the NFZ. Several situations may occur: (i) the disclosed location lies outside of the NFZ, and also the actual location lies outside of the NFZ—this is a True Negative (TN); (ii) the disclosed location is inside of the NFZ, but the actual location lies outside of the NFZ—this is a False Positive (FP); (iii) the disclosed location lies outside of the NFZ, but the actual location is inside the NFZ—this is a False Negative (FN); and finally, (iv) the disclosed location is inside the NFZ, and also real location lies inside the NFZ—this is a True Positive (TP). Moreover, when detecting a disclosed location inside the NFZ, the CI operator has to know the actual location to verify the invasion and possibly take action. However, the actual location of the UAV has not been disclosed. In turn, such situations would have a significant impact, as UAVs inadvertently invading the NFZ might cause severe safety and operational issues. Therefore, protecting drones' location privacy while allowing CI providers to detect invasions and take drones down is challenging and requires the design of a tailored solution. We remark that, for this use case, we consider benign drones unintentionally invading the NFZ. Malicious drones, intentionally invading the NFZ to cause damage, cannot be detected by relying only on RID messages, since malicious drone operators might easily stop transmitting RID messages. Conversely, the aim of this use case is to investigate the trade-off between location privacy and utility for benign drones.

**Use Case 2: Discovery of the closest Charging Station.** Consider a Service Provider (SP) managing a charging support system for Electric Vehicles (EVs) consisting of a group of *Charging Stations*. The SP distributes several charging stations in a given area and allows any EVs, including drones, to recharge by paying a fee. We consider that charging stations can receive RID messages and communicate with a central server online. Considering all the charging stations that received RID messages from a given UAV, being the only entity knowing the exact location of the control stations, the central server can determine the nearest control station to the UAV disclosed location. A control station can communicate with UAVs, e.g., through a secure communication link.

Consider a UAV on a mission, implementing location obfuscation to achieve location privacy. During the mission, the UAV needs to find the closest charging station to recharge its battery. As the UAV discloses an obfuscated location through RID messages, the central server of the charging support system can compute the nearest charging station only based on the disclosed location, not the actual one (this is never disclosed). As a result, the system might not be able to suggest to the UAV the charging station closest to the UAV's actual location. A sub-optimal choice can cause extra distance to be travelled by the drone and more energy consumption, possibly leading to battery drain, energy exhaustion and mission failure. Therefore, protecting drones' location privacy while allowing SPs to provide service is challenging and requires the design of a tailored solution. We remark that the aim of this use case is to investigate the trade-off between location privacy and utility for drone-based LBS. Real charging stations might also use a different protocol, e.g., broadcasting their own location so to allow

UAV to determine the best charging station autonomously. However, since no trade-off would be involved in such a scenario, we do not consider it for our analysis.

**Use Case 3: Drone-as-a-Service.** We consider drones deployed by a telecommunication SP and providing a service to users nearby, in line with the emerging Drone-as-a-Service (DaaS) scenario [19]. In particular, we assume such drones are equipped with a Subscriber Identity Module (SIM) card that allows them to connect to the mobile cellular network, relaying requests coming from active users. Thus, users without Internet connectivity in remote regions can connect to such UAVs, establish a secure connection, and make phone calls or access services available online.

Consider that the drones implement location obfuscation to achieve location privacy. Thus, when users would like to use a service provided by the SP via the drones, they connect to the Radio Frequency (RF) interface (WiFi), detect all UAVs in a given area and pick the one whose disclosed distance (via RID) is the least from the user location, assuming the closest drone is the one providing the best signal quality. As the UAVs disclose obfuscated locations, the user might make a sub-optimal choice, i.e., pick the UAV whose actual location is not the least. Thus, the signals emitted by the user and the UAV have to travel extra distance than the minimum, with consequent degradation of the achievable Quality of Service (QoS). Therefore, protecting a drone's location privacy while allowing a SP using such drones to provide reliable and efficient location-based services is challenging and requires the design of a tailored solution.

Note that users of DaaS applications might also use other parameters to pick the best UAV (e.g., the Received Signal Strength-RSS). However, channel quality indicators such as the RSS notoriously exhibit fast-fading phenomena that make distance estimation highly error-prone [20].

### 3.4 Requirements

From our previous discussion, we can extract a list of requirements for our proposal. These requirements can serve as a baseline to evaluate the applicability of different state-of-the-art techniques to our problem (see Sec. 4) and to assess the overall system performance (see Sec. 8).

- **R1: Location Obfuscation.** The latitude, longitude, and altitude reported by the UAV through RID messages must be obfuscated from takeoff to shutdown, i.e., its value should never be disclosed in plaintext.
- **R2: Trajectory Privacy.** A passive eavesdropper must not be able to use temporal correlation in the disclosed locations to extract the real UAV location from the obfuscated location released in RID messages.
- **R3: No Persistent Internet Connection on Drones.** The method to obfuscate the location should work on the UAV independently from the availability of a persistent Internet connection onboard.
- **R4: Maximum Messages Generation Time.** To keep compliance with the RID regulation, the time necessary to generate a RID message including an obfuscated location should not exceed 1 second.
- **R5: Maximum Communication Overhead.** The communication overhead resulting from the introduction of location obfuscation should not lead to message

fragmentation, due to the low reliability of broadcast communications and limited energy budget. Thus, RID messages should not exceed the Maximum Transmission Unit (MTU) of WiFi, i.e., 2,304 B [21].

#### 4 RELATED WORK

Several contributions in the current literature investigate location privacy issues and protection mechanisms in the context of vehicular networks. Some contributions provide location privacy via anonymity, as it can make tracking more difficult. One way to provide location privacy via anonymity is via pseudonyms [22], [23], i.e., short-term identifiers that keep changing on a (regular) time basis. Note that if an adversary knows the location and the time before the pseudonym changes, they can link the old pseudonym to the new one, breaking location privacy.

In the avionic domain, Sampigethaya et al. [24] propose to create areas dedicated to pseudonym swap where aircraft do not transmit messages, making it harder for a passive adversary to track aircraft based on wireless transmissions. This strategy cannot apply to our scenario, as drones should comply with RID. Svaigen et al. [25] propose creating dummy data and mobile entities. When applied to our context, these techniques would break compliance with RID and cause extra energy consumption.

Location privacy can also be achieved via location obfuscation, i.e., perturbing the location disclosed to other parties to prevent precise location tracking [26]. Geo-Indistinguishability is a well-known location obfuscation method proposed by Andres et al. [27], which protects the user's location over multiple location disclosures. Such an approach also preserves location utility to LBSs. Geo-Indistinguishability was designed for low-frequency location disclosure with no time correlation. The achievable location privacy decreases when sending messages frequently [28], as passive attackers can reveal the actual location through inference attacks [9]. Thus, many contributions extend Geo-Indistinguishability to face such inference attacks in various scenarios. Chatzikokolakis et al. [8] focus on supporting location traces for Geo-Indistinguishability. Their proposal reduces the computation cost by reusing noise, providing enough privacy for an entire day. However, they only used a limited number (30) of daily queries. Hua et al. [29] focus on reporting obfuscated locations in rapid succession. The proposed mechanism can work in both a basic and advanced mode. Such proposals assume an external trusted service computes the obfuscated location, so it does not apply to our scenario. As discussed by Svaigen et al. in [22], another option includes not revealing the exact location but the one of an entity somewhere in an area. The security and utility of such a system depend on the size of the site. Another option discussed by Svaigen et al. in [22] is to use a protocol that works on a node-to-node basis, which is also not an option if the drone is not working in a swarm. Sampigethaya et al. [24] also propose using cooperative schemes, which is inapplicable to our problem. Other proposed mechanisms either require time and energy-consuming computations before using the system, such as the one by Zhang et al. [30], or have a chance to release the actual location, such as the one by Xiong et al. [31], which

cannot fulfil our requirements. Xiao et al. [9], [32] specifically focus on the temporal correlation between location reports. They use a  $\delta$ -location set to protect the areas where the entity is most likely and develop an obfuscation method, namely Planar Isotropic Mechanism (PIM), which supports frequent location releases through a lightweight location obfuscation mechanism. Cao et al. [33] combine Geo-Indistinguishability with the proposal by Xiao et al. [9] and focus on obfuscating specific events, i.e. "moving between two specific places". Through this strategy, an adversary cannot tell if an event has occurred. However, such a method cannot protect trajectory privacy. In the drone context, a recent work by Enayati et al. considered the application of Laplacian Geo-Indistinguishability to protect UAV location privacy in goods delivery applications and drone-IoT applications [34]. However, the authors do not consider compliance with RID regulations. To sum up, we cross-compare in Tab. 1 the described techniques and evaluate if and how they fulfil our requirements (Sec. 3.4).

TABLE 1

Comparison of state-of-the-art techniques for location privacy regarding our requirements of interest discussed in Sec. 3.4. The symbol ● indicates that the paper fulfils the requirement, and ○ indicates that the paper does not address the requirement. In contrast, ◐ indicates partial fulfilment of the requirement (explanation in text).

Ref.	R1	R2	R3	R4	R5
[8]	◐	○	●	○	●
[9]	◐	●	●	○	●
[11]	●	◐	●	○	●
[22]	◐	○	○	○	●
[24]	◐	●	○	○	●
[27]	◐	○	●	○	●
[29]	◐	●	○	●	●
[30]	◐	●	●	○	●
[31]	◐	○	●	○	●
[33]	◐	○	●	○	●
[34]	◐	◐	●	○	●
OLO-RID	●	●	●	●	●

Note that none of the available solutions fulfils all our requirements, at the same time, motivating our work. The proposals which fulfil most of our requirements are the ones by Xiao et al. [9], [11], [29], and [30]. Some approaches cannot be improved to deal with trajectory privacy (e.g., [11]), while others cannot run on drones due to heavy computational demands( [29] and [30]). As for the proposal by [9] et al., it has not been conceived for 3D scenarios, it has not been tailored to constrained drones, and no considerations about their utility in drone-based scenarios have been provided. We integrate such an approach into our proposed solution as it achieves the lower bound of location privacy in equivalent 2-D scenarios. We will describe the integration process, extension, and evaluation in the following sections.

## 5 OLO-RID

### 5.1 Location Obfuscation on RID-enabled Drones

Our solution, namely OLO-RID, leverages the mathematical model of the PIM approach proposed by Xiao et al. in [9]. We first review the original approach and then discuss its limitations and our contributions.

**Introduction to PIM.** For ease of discussion, consider a two-coordinate system (latitude-longitude). We divide

the area around the moving entity into multiple cells  $s_1, s_2, \dots, s_N \in S$ . Based on previous travel data of the mobile entity or public data about such a journey, PIM requires us to create a transition matrix  $\mathbf{M}$ , holding the probability that the mobile entity moves from one cell to another. We denote  $M_{ij}$  as the probability that the mobile entity moves from cell  $i$  to cell  $j$ . We also consider a probability array  $\mathbf{p}$ , indicating the probability that the moving entity is in the cell  $s_i$ . As an example, if the mobile entity has a uniform probability of residing in cells 1, 2, 3, and 4, then  $p = [0.25, 0.25, 0.25, 0.25, 0, 0, \dots]$ . We define  $p_t^-$  as the prior probability at timestamp  $t$ , i.e., the probability that at time  $t$ , before a location release, the moving entity resides in a given cell. We also define  $p_t^+$  as the posterior probability, i.e., the probability that at time  $t$ , after a location release, the moving entity resides in a given cell. According to PIM, we compute the prior probability as  $p_t^- = p_{t-1}^+ \mathbf{M}$ . We can also compute the posterior probability according to Eq. 1, where  $\mathbf{z}_t$  is the location released at time  $t$ , and  $\mathbf{u}_t$  is the actual location.

$$p_t^+[i] = \frac{Pr(\mathbf{z}_t | \mathbf{u}_t = s_i) p_t^-[i]}{\sum_j Pr(\mathbf{z}_t | \mathbf{u}_t = s_j) p_t^-[j]}. \quad (1)$$

For a timestamp  $t$ , given the prior probabilities of the mobile entity's location  $p_t^-$  and the cells  $s_i \in S$ , we define the  $\delta$ -location set  $\Delta X$  as per Eq. 2.

$$\Delta X_t = \min\{s_i | \sum_{s_i} p_t^-[i] \geq 1 - \delta\}. \quad (2)$$

Consider the actual location of the mobile entity  $\mathbf{x}$ . The PIM mechanism aims to generate the obfuscated location offset  $\mathbf{z}^\#$ , s.t.  $\mathbf{z} = \mathbf{x} + \mathbf{z}^\#$ . To this aim, PIM applies the following procedure. We compute the convex hull from the  $\delta$ -location set  $\Delta X$ . Given a set of points and drawing lines between each point, the convex hull is the smallest area not crossing any line [9]. Denote a vertex of the convex hull as  $v_i$ . We denote  $\Delta V$  as the set of all values  $v_i - v_j$  for all possible  $i$  and  $j$ . From this, we calculate the sensitivity hull  $K$  of a convex hull of  $\Delta V$ . A sensitivity hull is a convex hull capturing the sensitivity between two releases from two instances, i.e., the difference between two queries if one piece of data has changed. From the sensitivity hull  $K$ , we sample points uniformly. These points are used in an isotropic transformation, resulting in the matrix  $T$ . To calculate the isotropic position from  $K$ , we get  $\mathbf{K}_I = T K$ . We sample from  $\mathbf{K}_I$  a point uniformly at random, namely  $\mathbf{z}'$ . To increase randomness, we use a Gamma distribution  $\Gamma(3, \epsilon^{-1})$  to get  $r$ . We denote the new random location as  $\mathbf{z}^* = r \cdot \mathbf{z}'$ . This point has to be transformed back to the original space  $\mathbf{z}^\# = T^{-1} \mathbf{z}^*$ . Finally, we can calculate our obfuscated location  $\mathbf{z}$  using the real location  $\mathbf{x}$  and  $\mathbf{z}^\#$ , thus we get  $\mathbf{z} = \mathbf{x} + \mathbf{z}^\#$ . Expanding the formula, we have that  $\mathbf{z} = \mathbf{x} + r T^{-1} \mathbf{z}'$ .

**Modifications to PIM.** As discussed in Sec. 4, the solution introduced by Xiao et al. in [9], namely PIM, does not fulfill all our requirements natively, preventing its straightforward integration for our problem. First, PIM protects the location in a two-dimensional coordinate system. However, UAVs move across a three-dimensional space. RID messages

still leak information when obfuscating only two dimensions, e.g., if the UAV is taking off or landing, leading to privacy issues. Thus, we extend the method by Xiao et al. to support location obfuscation in a 3-D space. Another downside of PIM when adopted in our context is the transition matrix, which contains a specific bounded area where the UAV is supposed to fly. When the UAV flies far outside these bounds, the computed obfuscated location is still based on a location within bounds, resulting in the computation of an obfuscated location very far from the actual location. In turn, such difference makes disclosed locations largely unrealistic. A naive solution could be uploading an extensive transition matrix on the UAV, so it likely always stays within bounds. However, a UAV is a constrained device with limited memory and computation power. Thus, loading an extensive transition matrix in memory is not an option. The computation time would also increase because of more extensive matrix computations. To solve this issue, our solution uses a small transition matrix supporting the areas around the UAV in all three dimensions. The drone gets information about the prior probabilities from publicly accessible or personal flight data. This is indeed feasible, as drones likely operate in well-defined areas, with limited size. In some cases, e.g., autonomous drones, the precise travel path is even known in advance. To generate the probabilities of a UAV flying from one cell to another, we initialise all the cells in the transition matrix to have the same probability  $\frac{1}{b^3}$ , in line with the logic of remotely piloted systems. Specifically, we check whether a cell near the UAV at timestamp  $t$  is also present at timestamp  $t-1$ . If true, the cell is regularly updated as  $p_t^- = M \cdot p_{t-1}^+$ . Otherwise, the value of  $p_t^- = M \cdot \frac{1}{b^3}$ . Algo. 1 provides the pseudo-code of our modified location obfuscation technique.

---

**Algorithm 1:** Extended PIM approach for location obfuscation in OLO-RID.

---

**Require:**  $\epsilon_t, \delta, \mathbf{M}, \mathbf{p}_{t-1}^+, \mathbf{x}_t^*, o_x, o_y, o_z, \mathbf{S}_{t-1}^\#, b$   
1  $\mathbf{o} = \text{Permute}([0, 1, -1]) [o_x, o_y, o_z];$   
2  $\mathbf{S}_t^\# = \mathbf{x}_t^* + \mathbf{o};$  // location offsets  
3  $\mathbf{p}_\# = [\frac{1}{b^3}, \dots, \frac{1}{b^3}];$   
4 **for any two location  $i, j$  in  $\mathbf{S}_t^\#$  and  $\mathbf{S}_{t-1}^\#$ , respectively do**  
5     **if  $i \approx j$  then**  
6          $p_\#[i] = p_{t-1}^+[j]$   
7     **end**  
8 **end**  
9  $\mathbf{p}_t^- \leftarrow \mathbf{p}_\# \cdot \mathbf{M};$   
10 **if location needs to be released then**  
11     Construct  $\Delta X_t;$  //  $\delta$ -location set  
12     **if  $\mathbf{x}_t^* \notin \Delta X_t$  then**  
13          $\mathbf{x}_t^* \leftarrow \tilde{x}_t;$  // surrogate  
14     **end**  
15     // release  $\mathbf{z}$   
16      $\mathbf{z} \leftarrow \mathbf{x}^* + r T^{-1} \mathbf{z}';$   
17     Derive posterior probability  $p_t^+$  by Equation 1;  
18 **end**  
19 **return** Algorithm 1 ( $\epsilon_{t+1}, \delta, M, p_t^+, x_{t+1}^*, S_t^\#$ )

---

We remark that the probability that the drone re-initializes the values of the prior probabilities to the default

value ( $\frac{1}{b^3}$ ) can be made arbitrarily small based on the knowledge of the area where the UAV has to fly and the autonomy of the battery deployed onboard.

## 5.2 OLO-RID Protocol flow

OLO-RID involves a *Registration Phase*, executed before drone deployment, and a *Runtime Phase*, executed during deployment. Fig. 1 provides an overview of the operations required in such two phases, as described below.

- 1 To start the *Registration Phase*, the *UAV operator* and the *TTP* establish a secure connection over the Internet, e.g., through TLS, to register the UAV. Such a registration only happens once for a given UAV.
- 2 The *UAV operator* retrieves the Unique Identifier (UID) from the UAV, and specifically, from the *RID Module*.
- 3 The *UAV operator* delivers *UID* to the *TTP* through the secure connection.
- 4 The *TTP* stores *UID* in the Public Information Registry (PbIR), for future use.
- 5 The *TTP* delivers to the *UAV operator* the public key  $pk_{USS}$ , through the secure connection.
- 6 The *UAV operator* installs the key  $pk_{USS}$  onto the UAV, to be used later on in the *Runtime Phase*. The *Registration Phase* ends here.
- 7 The *Runtime Phase* is executed at runtime every time the UAV needs to create a new RID message. In particular, the *RID Module* on the UAV first requests the current location to the *GNSS Module* onboard.
- 8 The *GNSS Module* extracts the UAV's location  $x$  and velocity  $v$  and delivers them to the *RID Module*.
- 9 The *RID Module* on the UAV sends the location  $x$  and the public key  $pk_{USS}$  to the *Encryption Module*.
- 10 The *Encryption Module* encrypts the location  $x$  using the ECIES scheme (Sec. 2) as  $c = PKE.ENC(x_{lat}||x_{lon}||x_{alt}, pk_{USS})$ , and sends it back to the *RID Module*.
- 11 The *RID Module* sends the location  $x$  to the *Obfuscation Module*.
- 12 The *Obfuscation Module* generates an obfuscated location  $z$  from the location  $x$ , as  $z = PIM(x)$ , and sends it back to the *RID Module*.
- 13 The *RID Module* generates a RID message  $m$  using the UID, obfuscated location  $z$ , velocity  $v$ , CS's location  $x_{CS}$ , the current timestamp  $t$ , the emergency status at time  $t$   $em_t$ , and the encrypted location  $c$ , as  $m = UID||z||v||x_{CS}||t||em_t||c$ .
- 14 The UAV broadcasts the RID message over the wireless channel.

## 5.3 Application of OLO-RID in Reference Use Cases

In this section, we describe how the services connected to the use cases described in Sec. 3.3 can use the location disclosed by the drones via OLO-RID.

**Use Case 1: Invasion of No-Fly Zone.** Consider a RID-equipped UAV is approaching a NFZ, monitored by a *CI Monitoring Station (MS)*. We show the protocol flow in this use case in Fig. 2 while describing the steps below.

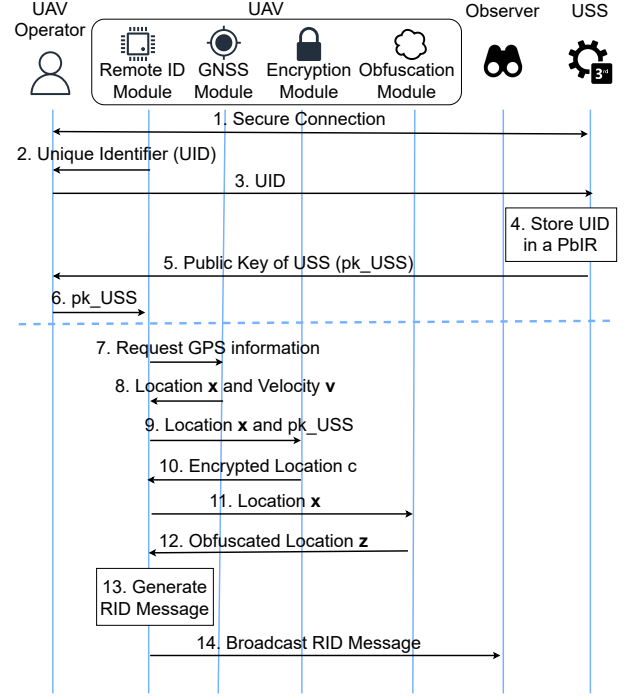


Fig. 1. Sequence diagram of the operations required for the *Registration Phase* (upper part) and *Runtime Phase* (lower part).

- 1 In the *Registration Phase*, the *CI MS* and the *TTP* establish a secure connection over the Internet, e.g., through TLS, to register the bounds of the NFZ for further usage. Such a registration must only happen once for a given *CI*.
- 2 The *CI MS* delivers the NFZ bounds to the *TTP* to register the NFZ.
- 3 The *TTP* stores the received NFZ bounds in a the Private Information Registry (PvIR) for further usage.
- 4 The *TTP* delivers an acknowledgement message back to the *CI MS*, to confirm bounds registration. This operation ends the *NFZ Registration Phase*.
- 5 At runtime, the *UAV* broadcasts a RID message through the *RID module*, as discussed above.
- 6 The *CI MS* receives the RID message and checks whether the obfuscated location is within the bounds of the NFZ. The protocol flow described here continues only if the obfuscated location reported by the UAV is within the NFZ.
- 7 The *CI MS* and the *TTP* establish a secure connection over the Internet (e.g., via TLS) to exchange data about the UAV's location.
- 8 The *CI MS* forwards the message received from the UAV to the *TTP*.
- 9 The *TTP* decrypts the encrypted location report  $c$  in the received message  $m$ , using its private key  $sk_{USS}$  and the ECIES algorithm, as  $x = PKE.DEC(c, sk_{TTP})$ , so retrieving the UAV's actual location. The following actions depend on whether the UAV is actually invading. When the UAV invades the NFZ, we report the steps below with an 'a'. Otherwise, we report them with a 'b'.



- 10a If the UAV is actually invading the NFZ, the *TTP* delivers the UID and the plaintext location of the UAV  $x$  to the *CI MS*.
- 11a The *CI MS* takes action against the UAV.
- 10b If the UAV is not invading, the *TTP* sends only the UID to the *CI MS*. It never reveals the plaintext location, protecting the UAV's location privacy.

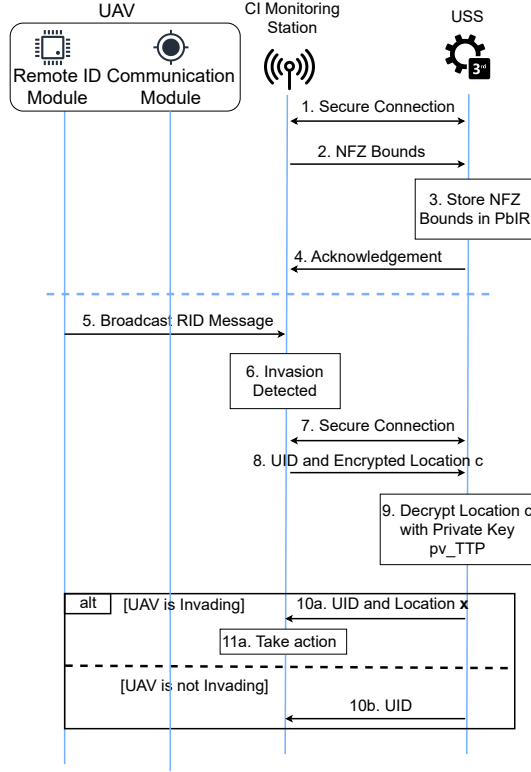


Fig. 2. Sequence diagram of the operations executed in Use Case #1 to register the NFZ (upper part) and handle a RID message on the observer (lower part).

**Use Case 2: Discovery of the closest Charging Station.** Consider a RID-enabled UAV looking for the closest charging station. We show the protocol flow for this use case in Fig. 3 while we describe the required steps below.

- 1 In the *Registration Phase*, each *Charging Station  $j$*  and the *CS* establish a secure connection over the Internet, e.g., through TLS, to register the location of the *Charging Station*. Such a registration only happens once for a given *Charging Station*.
- 2 The *Charging Station  $j$*  delivers its location  $x_{CS,j}$  to the *Central Service* to store the location.
- 3 The *Central Service* stores the location of the *Charging Station* in the *PvIR*, for later usage.
- 4 The *Central Service* sends an acknowledgement message back to the *Charging Station  $j$* , to acknowledge correct operations, so ending the *Registration Phase*.
- 5 At runtime, the *UAV* broadcasts a RID message through the *RID module*, as discussed above.
- 6 *Charging Station 1* receives the RID message containing the UAV (obfuscated) location  $z$  and forwards it to the *Central Service*.

- 7 *Charging Station 2* receives the RID message containing the UAV (obfuscated) location  $z$  and forwards it to the *Central Service*.
- 8 The *Central Service* compares the location  $z$  reported by the UAV to the locations of all the *Charging Stations* receiving such a message, i.e.,  $x_{CS,1}$  and  $x_{CS,2}$ , and determines the UID of the one which is the best to serve the request by the UAV, as  $UID = i : \min_i(|z - x_{CS,i}|)$ .
- 9 The *Central Service* sends the UID  $i$  back to the *Charging Station* that is closest to the UAV.
- 10 The nearest *Charging Station* establish a connection with the communication module on the UAV.
- 11 The nearest *Charging Station* sends its location to the UAV, so that it can recharge its battery.

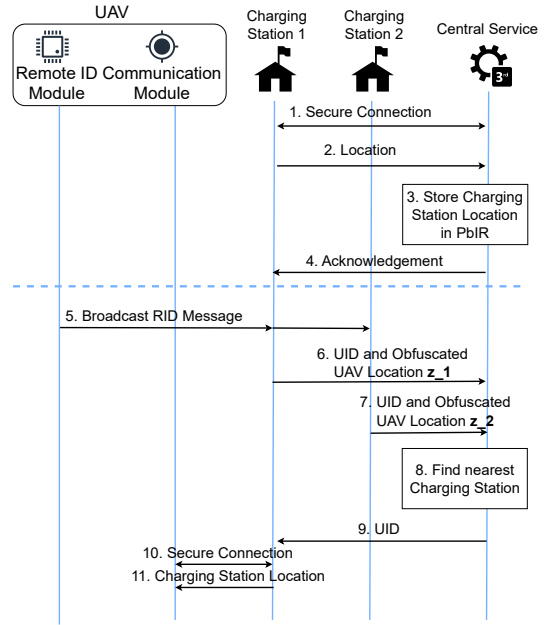


Fig. 3. Sequence diagram of the operations executed in Use Case #2 to register charging stations (upper part) and handle a RID messages on the observers (lower part).

**Use Case 3: UAV as a Service.** Consider a RID-enabled UAV offering telecommunications services. We show the protocol flow for this use case in Fig. 4 while we describe the required steps below. We omit the Registration phase since there are no changes compared to Fig. 1.

- 1 UAV 1 broadcasts a RID message through the local *RID Module*, reporting its obfuscated location  $z_1$ .
- 2 UAV 2 broadcasts a RID message through the local *RID Module*, reporting its obfuscated location  $z_2$ .
- 3 Consider a user receiving several RID messages. It picks the nearest UAV based on the reported obfuscated location.
- 4 The user and the nearest UAV, e.g. UAV 1, establish a secure connection.
- 5 The user can send and receive data to and from UAV 1, so using its services.



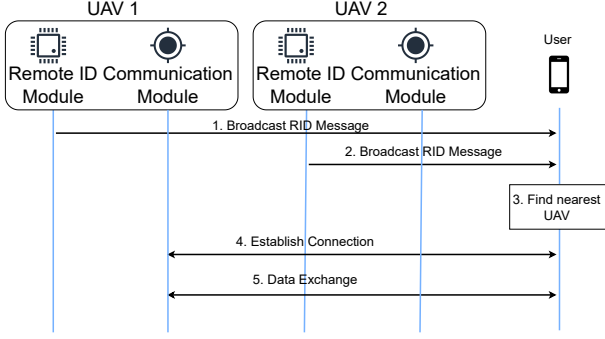


Fig. 4. Sequence diagram of the operations executed in Use Case #3 to find the nearest UAV providing services.

## 6 SECURITY ANALYSIS

In this section, we discuss the main security features offered by our solution.

**Location Obfuscation Privacy.** Our solution integrates the approach proposed by Xiao et al. in [9] to disclose an obfuscated location  $\mathbf{z}$  in place of the current UAV location  $\mathbf{x}$ . As noted by relevant works on location privacy [8], achieving complete location privacy when frequently disclosing the current location is not feasible. However, as demonstrated by Xiao et al. in [9], the proposed solution achieves the lower bound of trajectory privacy when considering multiple time-correlated location disclosures.

As per the introduced modifications to the method by Xiao et al., we first notice that we apply location obfuscation on a 3-D space. As we use the algorithm independently on the horizontal (latitude and longitude) and vertical coordinates (altitude), such a change does not impact the location privacy of the single coordinates. Our proposed OLO-RID solution also modifies the computation of the prior probability array ( $p_t^-$ ). Specifically, we generate all permutations of  $[0, 1, -1]$  and create a box around the current UAV location, consisting of  $b^3$  cells, where  $b$  denotes the number of cells in each dimension. Recall that UAVs can move in space across consecutive location disclosures. Thus, such a movement may lead to the generation of new cells if the UAV moves into a new cell. In OLO-RID, we minimize the probability of this event through the knowledge of the area where the drone is flying. When this change occurs, OLO-RID re-initialize all cells to  $p_{\#} = \frac{1}{b^3}$ . As per [9], we compute the prior probability as  $p_t^- = p_{\#}M$ , being  $M$  the transition matrix. We recall the definition of adversarial privacy [9].

**Definition 2. (Adversarial-privacy).** A mechanism is  $\epsilon$ -adversarially private if for any location  $\mathbf{s}_i \in \mathbf{S}$ , any output  $\mathbf{z}$  and any adversary knowing the true location is in  $\Delta X$ :

$$\frac{Pr(u_t^* = s_i | z_t)}{Pr(u_t^* = s_i)} \leq e^{\epsilon} \quad (3)$$

where  $Pr(u_t^* = s_i)$  and  $Pr(u_t^* = s_i | z_t)$  are the prior and posterior probabilities of any adversaries.

In our setting, adversarial privacy is equivalent to differential privacy on the  $\delta$ -location, as shown by Xiao et al. [9]. Thus, we can re-use the same proof in Xiao et al. [9].

**Theorem 1.** At any timestamp  $t$ , Algorithm 1 is  $\epsilon_t$ -differentially private on 0-location set.

*Proof.* It is equivalent to proving adversarial privacy on a 0-location set, which includes all possible locations. If  $x_t^* \in \Delta X_t$ , then  $z_t$  is generated by  $x_t^*$ . As shown by Xiao et al. [9],  $z_t$  is  $\epsilon_t$ -differentially private. So  $\frac{Pr(u_t^* = s_i | z_t)}{Pr(u_t^* = s_i)} \leq e^{\epsilon}$ . When  $x_t^* \notin \Delta X_t$ , we can replace  $x_t^*$  with a surrogate  $\tilde{x}_t$ , and thus:

$$\frac{Pr(u_t^* = s_i | z_t)}{Pr(u_t^* = s_i)} = \frac{\sum_k Pr(u_t^* = s_i | \tilde{x}_t = s_k) Pr(\tilde{x}_t = s_k | z_t)}{\sum_k Pr(u_t^* = s_i | \tilde{x}_t = s_k) Pr(\tilde{x}_t = s_k)} \leq e^{\epsilon} \quad (4)$$

Therefore, being the framework adversarially private, Algorithm 1 is also  $\epsilon_t$ -differentially private on 0-location set.  $\square$

**Encrypted Location Report Robustness.** OLO-RID requires delivering encrypted location reports, i.e., cryptography values allowing the TTP (USS) to obtain the plain-text drone location, if necessary. To do so, we use the ECIES public-key encryption scheme, implying the generation of an ephemeral symmetric key signed through the public key of the USS. Such location reports can only be decrypted using the private key of the USS, which is assumed to stay private on the USS throughout the deployment of the system. If the private key of the USS is not leaked, based on the cryptographic properties of ECIES, a passive eavesdropper cannot obtain the plain-text location  $\mathbf{x}$  used to generate the ciphertext  $c$ . The eavesdropper cannot even know if the plain-text location  $\mathbf{x}$  changes or stays the same across consecutive location disclosures, thanks to the protection offered by ECIES against chosen-ciphertext, and chosen-plaintext attacks, as discussed in [15].

## 7 PROOF-OF-CONCEPT IMPLEMENTATION

We implemented two PoC of OLO-RID, as described below.

**Hardware Details.** We use two different devices as a drone, i.e., a general-purpose laptop and an embedded device, to evaluate the performance of OLO-RID on high-end and medium-end drones. Our first PoC uses a general-purpose laptop equipped with one CPU running at 2.60GHz and 16GB of Random Access Memory (RAM). Such features align with the resources available onboard medium-high-end drones, e.g., the DJI Matrice 300 [35]. The second PoC uses as the drone a RPI Model 3B+, featuring a 1.4GHz CPU and 1GB of RAM [36]. The resources available on the RPI align with the ones of medium-low-end drones such as the DJI Mini 2 [37]. Also, note that such a choice aligns with the methodology used by other scientific contributions in the drone security domain [19]. Note that both the laptop and the RPI integrate an IEEE 802.11b/g/n wireless module, useful for transmitting and receiving RID-compliant WiFi messages over the air.

**Software.** We implemented OLO-RID using the C programming language to reduce runtime delays deriving from language interpretation as much as possible. We used the well-known library MIRACL CORE to implement cryptography operations required by the ECIES encryption scheme [38]. Note that we chose MIRACL Core due to its well-known excellent performance on low-powered IoT systems and the available support for several elliptic curves, as required for running ECIES. Such a choice also aligns with relevant literature on security solutions for constrained

drones [6]. We report in Tab. 2 the Elliptic Curves (ECs) we used within the ECIES scheme. To show the difference between curves of the same security levels, we have also considered two additional curves, namely BN254 and BLS48556. Using such curves could give us information about the difference in performance between two curves with the same level of security. Note that the curve BN254 was designed for 128-bit security [39] but, recently, its actual security decreased to 100-bit [40].

TABLE 2  
ECC Curves features.

ECC Curve	Key size [B]	#-Bit Security
BN254	64	100 [40]
secp256r1 (NIST256)	64	128 [41]
secp384r1 (NIST384)	96	192 [41]
secp521r1 (NIST521)	132	256 [41]
BLS48556	140	256 [42]

As for the extended PIM solution integrated into OLO-RID, we first implemented the required operations using MATLAB© R2023a. Then, we used the tool *MATLAB Coder* to convert the code into C. We manually fixed a few post-conversion inconsistencies and then cross-compiled the code through *GCC* and *GNU make* to create a library able to run on the target hardware devices used in our PoC. Tab. 3 shows the message format of OLO-RID.

TABLE 3  
Modified RID message format in Bytes.

Content	Bytes [B]
Unique identifier	4
Obfuscated UAV longitude	4
Obfuscated UAV latitude	4
Obfuscated UAV altitude	4
UAV longitude velocity	2
UAV latitude velocity	2
UAV altitude velocity	2
CS longitude	4
CS latitude	4
CS altitude	4
Timestamp	4
Emergency status	1
Ephemeral key	64-140
Ciphertext	16
HMAC tag	32
Total	151-227

We ran OLO-RID on the RPI as a native process. Instead, on the general-purpose laptop, to isolate our protocol from concurrent processes as much as possible, we ran OLO-RID within a Linux-based virtual environment featuring 4 CPU cores and 8GB of RAM. The source code of our solution is available open-source at [10].

## 8 EXPERIMENTAL EVALUATION

### 8.1 Experimental Methodology

**Research Questions.** Our experimental assessment aims to answer the following Research Questions (RQs).

- **RQ1:** What is the runtime overhead of OLO-RID on regular drones regarding computation time, RAM usage, energy expenditure, and communication bandwidth with various security levels?

- **RQ2:** How can we improve the location privacy provided to the drone at runtime, and how do such improvements affect the overhead of our solution?
- **RQ3:** What is the utility of the location disclosed through OLO-RID by the drone across various configuration parameters while considering our reference use cases discussed in Sec. 3.3?

UAVs are constrained devices, characterized by (one or more) constraints regarding available computational, memory, communication bandwidth, and energy resources. Such constraints make it challenging to implement and run a suitable technique for location obfuscation while still creating and broadcasting RID messages within the time limitations imposed by the RID regulation (1 second). **RQ1** sets a baseline for the overhead of our solution when using different hardware and various ECs. **RQ2** investigates the impact in terms of location privacy and overhead on the drone derived by changing relevant location obfuscation parameters (i.e.,  $\epsilon$ ). Finally, **RQ3** evaluates OLO-RID in the specific context of our use cases (Sec. 3.3). We specifically focus on the trade-off between drone location privacy and utility, i.e., the extent to which drone-based LBSs can successfully use the disclosed location.

**Experiments Settings.** To answer the RQs above, we designed a measurement system to obtain the execution time, RAM usage, communication overhead, energy consumption, location privacy and utility of our approach. As for the execution time, we measured the time (in milliseconds) necessary to generate a RID message secured through OLO-RID, from the acquisition of the current location from the GNSS (not included) to the assembling of the entire RID message (wireless communication not included). We specifically excluded location acquisition and wireless communication as they are orthogonal processes to our solution, which might be executed asynchronously. As for the RAM usage, we used the Linux tool */usr/bin/time -v*, providing the maximum instantaneous RAM occupancy of a process. Through this tool, we can obtain an indication of the amount of RAM to be deployed on the involved devices to support our solution fully. As for the communication cost, using standard tools provided by default C libraries, we measured the size of the complete RID message after the application of our solution. We also measure the energy consumption (in millijoule) the drone requires to run our solution. To this end, in line with similar contributions, we used the energy estimation tool *powertop* provided by the Linux OS. *Powertop* estimates the power (in Watts) of a running process based on hardware-dependent power consumption figures. To compute the corresponding energy consumption  $E$ , we multiply the obtained power estimate  $P$  for the duration of the process of interest  $\Delta T$  (the duration of the runtime phase), measured as described above, as  $E = P \times \Delta T$ . Such a value can indicate the energy required to run our solution and, thus, the battery to be installed on the drone to keep broadcasting (location) privacy-preserving RID messages for the whole mission. To evaluate the location privacy provided to the drone thanks to the application of our solution, in line with the relevant literature [11], we use the *average distance*, i.e., the average value of the (absolute) difference between the actual drone

location and the disclosed (obfuscated) one. The higher the average distance, the more significant the uncertainty on the real drone's location, thus, the higher the location privacy. Finally, as for the utility of the drone's disclosed location, we ran simulations in Matlab using real drone traces (see below the reference dataset used in our analysis). We used metrics specific to the considered use case. For the use case #1, we considered the number of TPs (actual detected invasions of no-fly area), FPs (false detected invasions of no-fly area), TNs (correct identified non-invasions of the no-fly area) and FNs (missed detected invasions of the no-fly area) as seen by the invasion monitoring system. For the use case #2, we considered the *average extra distance*, i.e., the extra distance the drone has to travel to reach the suggested charging station compared to the distance to reach the optimal one. Finally, for the use case #3, we evaluate the *average extra distance* as the additional space the signal emitted from the suggested UAV has to travel to reach the user compared to the distance it would travel from the UAV closest to the requesting user.

**Reference Dataset.** In this work, for flight data of the involved drones, we use the actual flight dataset provided by NATO's Emerging Security Challenges Division [43], in line with similar works [11]. The data refer to multiple flights paths of various drones in an area of 1.5 km 72.6 km 740 m. For all the tests, we use the flight path shown in Fig. 5, including over 5,000 location disclosures in its flight path. Instead, for the analysis of the use cases, we use the flight path shown in Fig. 6, which includes over 8,000 locations. We used a different flight path to analyze the use cases so as to work in a controlled environment, where the UAV flies mainly in a straight line. Such a trajectory eliminates anomalies due to weird flight paths and makes it easier to reason about the entire scenario. We ran all tests at

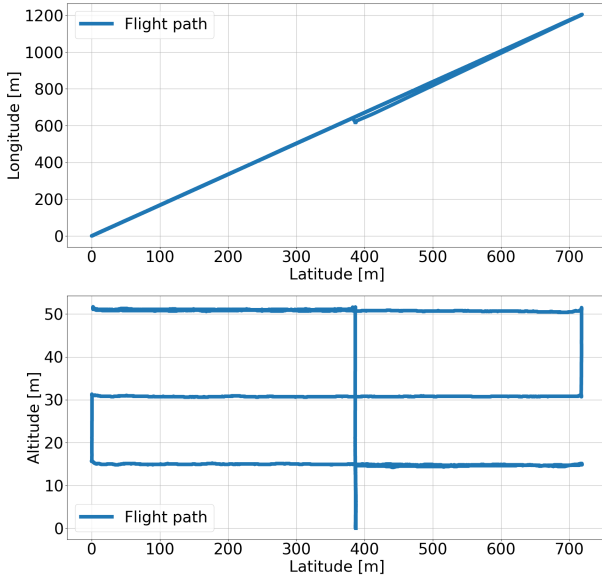


Fig. 5. Representation of the flight path used for the experiments in Sec. 8.2 and 8.3, with top-down and side view.

least 5,000 times, so as to average the results over multiple locations and trajectories. We also ran all tests using the highest privileges on the specific hardware, avoiding delays

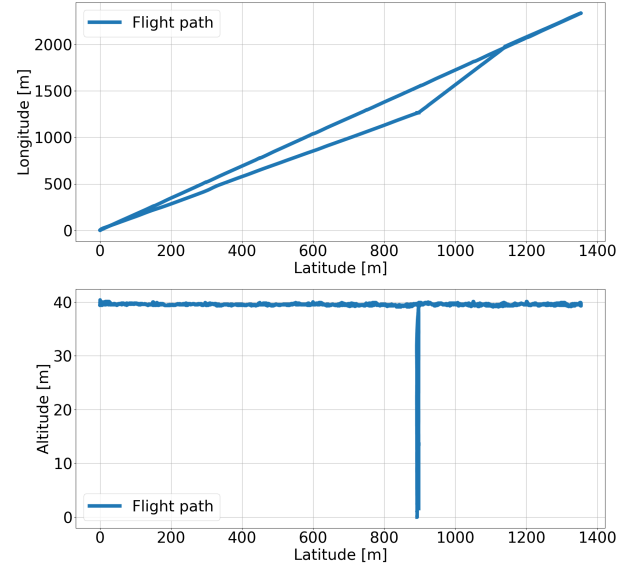


Fig. 6. Representation of the flight path used for the experiments in Sec. 8.4, with top-down and side view.

due to background concurrent processes. As a reference, we show in Fig. 7 the relationship between the actual drone path, the released obfuscated locations and the WiFi coverage (upper bound on the location privacy).

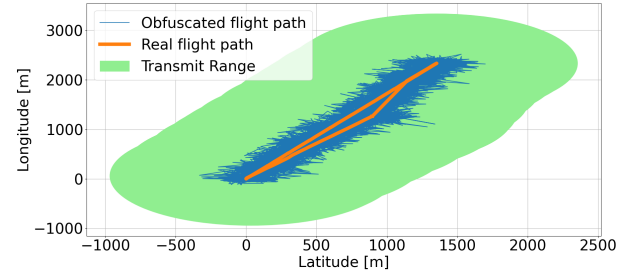


Fig. 7. UAV actual trajectory, obfuscated trajectory (with an average distance of 100 meters) and WiFi coverage of 1,000 meters.

## 8.2 Experiment 1: Overhead Evaluation

To answer **RQ1**, we measure the overhead of OLO-RID with different curves on a regular laptop and a RPI.

**Time.** Fig. 8 reports the average time (and 95% confidence intervals) required to create a RID message using OLO-RID. The upper figure shows the results of our tests on the laptop, while the bottom results are for the RPI.

As intuition would suggest, the average time required to run our solution increases with the size of the EC points (keys) used in the curve, i.e., with the provided security level. Considering the two curves NIST521 and BLS48556, both providing 256-bit security, we can see a slight discrepancy between the results obtained on the laptop and those obtained on the RPI. However, this difference is negligible (3.5 %), and it does not affect the rationale of our findings. It is essential to notice that all our results, both on the laptop and on the RPI, report execution times well below the

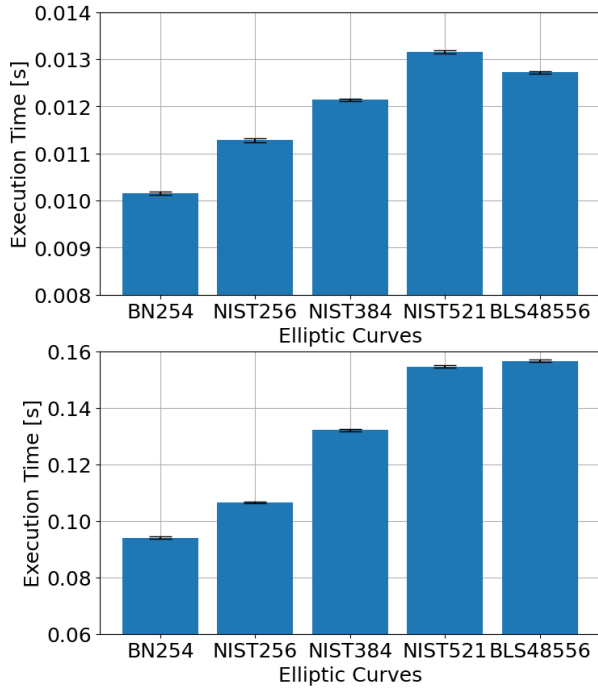


Fig. 8. Time required to run OLO-RID on a regular-laptop (up) and RPI (bottom), with 95% confidence interval.

threshold of 1 s. The minimal execution times demonstrate the viability of our solution on relevant hardware.

**RAM.** Fig. 9 reports the average peak RAM consumption of our solution, with 95% confidence intervals. We

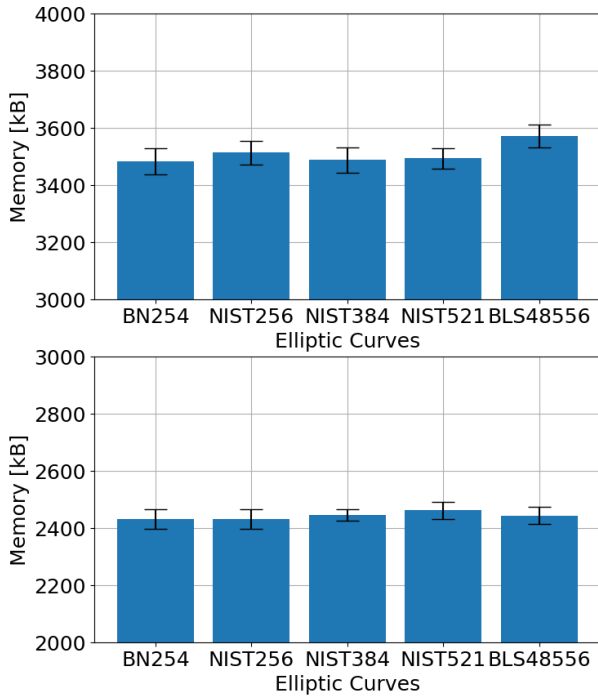


Fig. 9. RAM required by OLO-RID on the general-purpose laptop (upper figure) and RPI (bottom), with 95% confidence interval.

notice that, on the particular hardware platform, the RAM

consumption of our solution is independent of the chosen security level. On the laptop, our solution requires 3,600 kB of RAM in the worst case, which is very lightweight and affordable even on low-end drones. We highlight that it is not possible to cross-compare the RAM consumption on the two different platforms because the underlying memory management system of such platforms is different.

**Communication.** To evaluate the communication overhead of OLO-RID, we can compare the regular RID format with the RID message format required by our solution, summarized in Table 3. OLO-RID requires changing the content of three fields (current latitude, longitude, and altitude of the drone) and delivering three additional fields. The modified fields require the same amount of bytes as the regular fields, generating no additional overhead. As for the three added components, i.e., ephemeral key, ciphertext, and HMAC tag, the ciphertext and HMAC tag required by ECIES have a constant size of 16 and 32 bytes, respectively. The size of the ephemeral key depends on the adopted curve and, as per Tab. 2), it varies between 64 and 140 bytes. Thus, the total communication overhead of OLO-RID for a single message ranges between  $16 + 32 + 64 = 112$  Bytes and  $16 + 32 + 140 = 188$  Bytes. The maximum RID message size with OLO-RID amounts to 227 bytes, which is well below WiFi's MTU, i.e., 2,304 bytes [21].

**Energy.** Fig. 10 reports the average energy required by OLO-RID on both the laptop and the RPI, together with 95% confidence intervals. In line with Fig. 8, increasing the

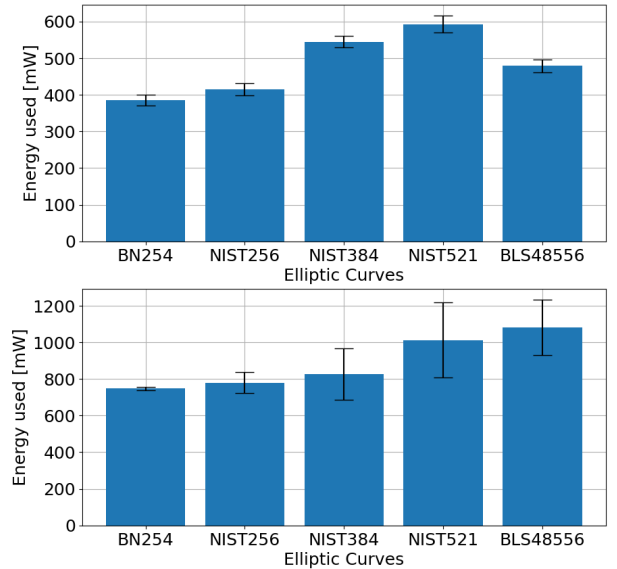


Fig. 10. Energy expenditure of OLO-RID on a regular laptop (upper figure) and Raspberry PI 3 (bottom), with 95% confidence interval.

number of security bits increases the energy consumption of our solution. The energy expenditure is primarily influenced by the time necessary to complete the protocol. We can notice the same difference between the curves NIST521 and BLS48556 among the two testbeds, as discussed above. The most energy-consuming curve on the laptop is NIST521, which requires 600 mJ for protocol run. The most energy-consuming curve on the RPI is BLS48556, which requires an average of 1,100 mJ per protocol run. We cannot cross-

compare the energy expenditure across different hardware platforms, due to the different components and voltage needed to power them. We discuss the impact of the measured energy expenditure on an average drone in Sec. 9.

### 8.3 Experiment 2: Privacy Analysis

For answering RQ2, we analyze the impact of  $\epsilon$  on the location privacy provided to the drone and the overhead incurred by OLO-RID. We recall from Sec. 5 that OLO-RID uses  $\epsilon$  to tune the privacy level of the extended PIM obfuscation mechanism. Tab. 4 reports the average distance of the disclosed location to the actual one for different values of the parameter  $\epsilon$ , with  $\delta = 0.01$ .

TABLE 4

Impact of the parameter  $\epsilon$  on the average distance between the actual UAV location and the disclosed (obfuscated) one, with  $\delta = 0.01$ .

$\epsilon$	Average Distance [m]
0.001	2533.38
0.005	506.65
0.01	253.37
0.05	50.72
0.1	25.35
0.5	5.06
1	2.54

Changing  $\epsilon$  affects the average distance significantly, from just a few meters (2.54 meters with  $\epsilon = 1$ ) to a few kilometres (2,533.38 meters with  $\epsilon = 0.001$ ). On the drone, lower values of  $\epsilon$  provide higher average distance values and, thus, more privacy. However, we have to consider also the utility of the disclosed location to LBSs. We analyze the utility of the disclosed locations in Sec. 8.4 while, in the rest of this analysis, we focus on three reference values of  $\epsilon$ , i.e., 0.01, 0.05, 0.1. Fig. 11 and Fig. 12 report the average time and the energy (with 95% confidence intervals) required to compute a RID message through our solution on the RPI with such values of  $\epsilon$ , respectively.

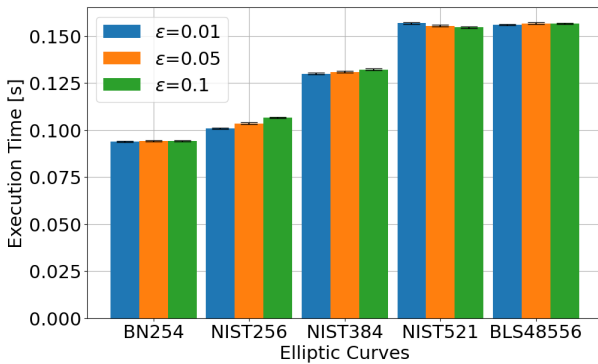


Fig. 11. Time required to compute a RID message with OLO-RID and various values of  $\epsilon$  on a RPI, with 95% confidence interval.

From Fig. 11, we can see no impact on the execution time when we change  $\epsilon$ . We notice minor changes among the different  $\epsilon$  values. In general,  $\epsilon = 0.1$  uses more energy than the others—in the worst case, 18% more. When looking specifically at the higher security ECs  $\epsilon = 0.01$  is more energy efficient. Overall, the trend found in Fig. 8 still applies, i.e., the EC curve used as part of ECIES is the most relevant

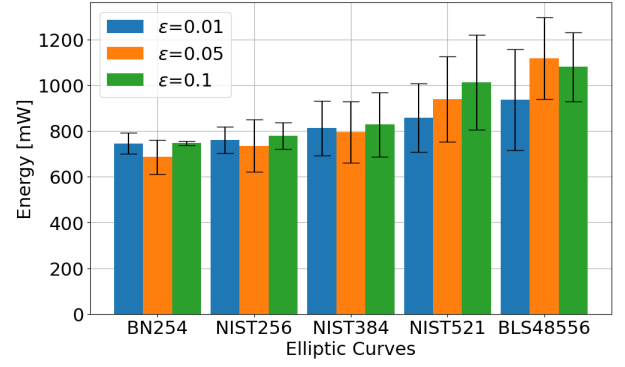


Fig. 12. Energy required to compute a RID message with OLO-RID and various values of  $\epsilon$  on a RPI, with 95% confidence interval.

source of energy consumption in the protocol. We also notice oscillating results when investigating the protocol's RAM consumption while varying  $\epsilon$ , as shown in Fig. 13. Here, we notice that choosing  $\epsilon = 0.1$  is always more memory-efficient than the other options, but with a small margin of 3%, while  $\epsilon = 0.01$  and  $\epsilon = 0.05$  approximately use the same amount of RAM. As all of the values of  $\epsilon$  report similar results, we believe the specific value of  $\epsilon$  does not affect the RAM overhead of our solution significantly.

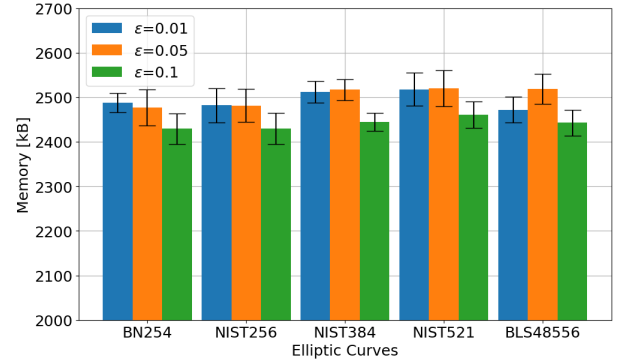


Fig. 13. Memory required to compute a RID message with OLO-RID and various values of  $\epsilon$  on a RPI, with 95% confidence interval.

### 8.4 Experiment 3: Use Cases

To answer RQ3, we consider each use case introduced and described in Sec. 3.3. For each of them, we identify utility criteria and investigate the impact of different protocol configurations on the utility of the disclosed location.

**Use Case 1: Invasion of No-Fly Zone.** Consider the Use Case 1 described in Sec. 3.3 and particularly, the scenario depicted in Fig. 14, where the big red circle represents the CI location, the straight black path represents the NFZ boundaries, the dotted black path represents the WA bounds, and the blue path identifies the drone path. Recall the definitions of TPs, FPs, TNs, and FNs given in Sec. 8.1. In general, we aim to have very high TPs and TNs, as well as very low FPs and FNs. However, as timely drone detection takes priority, we aim to keep the TPs high while reducing the FPs as much as possible. We consider two reference values for the



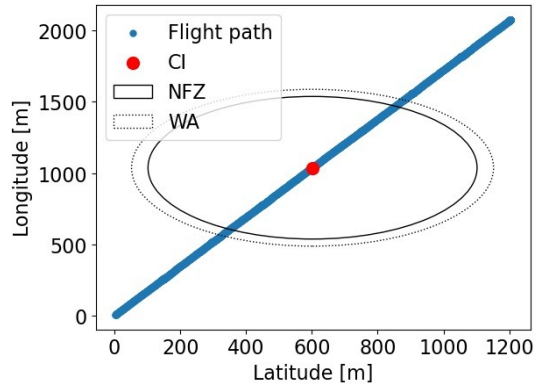


Fig. 14. Use Case # 1 analysis: sketch of the NFZ and WA surrounding a CI, with an actual drone flight path passing through.

average distance, i.e., 25 m and 100 m. We set the radius of the NFZ to 500 m, and we consider two values for the radius of the WA, i.e., 505 m and 600 m, to investigate to what extent the difference between the NFZ and the WA impacts our findings. Figs. 15 and 16 report the confusion matrices of the detection system considering the average distance of 25 m and the WA radius of 505 and 600 m, respectively. We

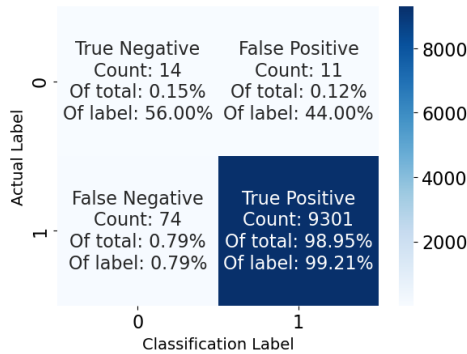


Fig. 15. Confusion matrix of the detection system in Use Case #1, considering a WA radius of 505 m and an average distance of 25 m.

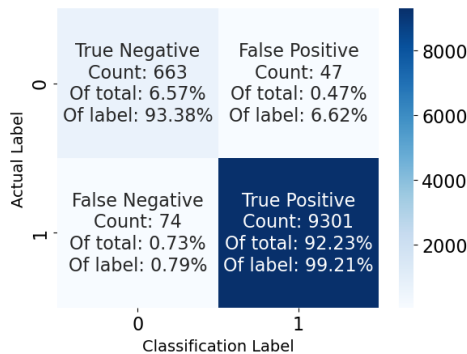


Fig. 16. Confusion matrix of the detection system in Use Case #1, considering a WA radius of 600 m and an average distance of 25 m.

notice that the size of the WA does not impact the TPs, while it does affect the FPs. In fact, increasing the radius of the

WA, even though the percentage of FPs decreases, the actual number of FPs increases. Considering that each FP involves an interaction over the Internet between the CI observer and the USS (see Sec. 5.3), the CI operator can choose a small WA, characterized by a radius similar to the one of the NFZ, so as to reduce FPs and, accordingly, the required interactions with the USS. We can notice the trend described above also when comparing Figs. 17 and 18, considering the same analysis as above but with an average distance of 100 m in the locations disclosed by the drone. Increasing the average distance to 100 m increases the FNs significantly compared to using an average distance of 50 meters, thus increasing the chances that the CI misses an invading drone. At the same time, with an average distance of 100 m, the FPs also increase, as there are more chances that a drone which is not invading discloses a location inside the NFZ, thus falsely resulting as invading. To decrease the number of FPs, the WA should be as small as possible. While increasing the average distance increases FNs, there are more chances that the invasion is detected within a few seconds, resulting in a TP. Also, when the WA is small, increasing the average distance barely affects the number of FPs.

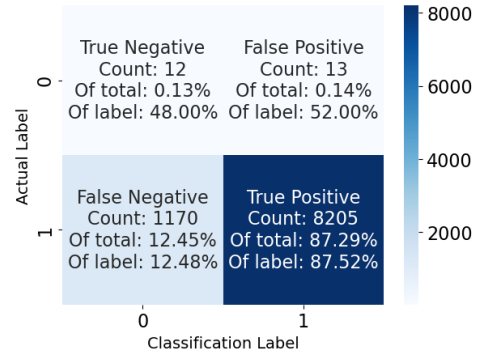


Fig. 17. Confusion matrix of the detection system in Use Case #1, considering a WA of 505 m radius and an average distance of 100 m.

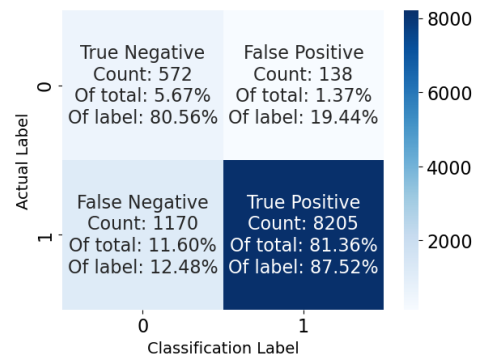


Fig. 18. Confusion matrix of the detection system in Use Case #1, considering a WA of 600 m radius and an average distance of 100 m.

### Use Case 2: Discovery of the closest Charging Station.

Consider the Use Case 2 described in Sec. 3.3, and particularly, the scenario depicted in Fig. 19, where an UAV is moving in area where 8 charging stations are deployed.

Without OLO-RID, the system would suggest to the UAV the nearest charging station to the actual UAV location.

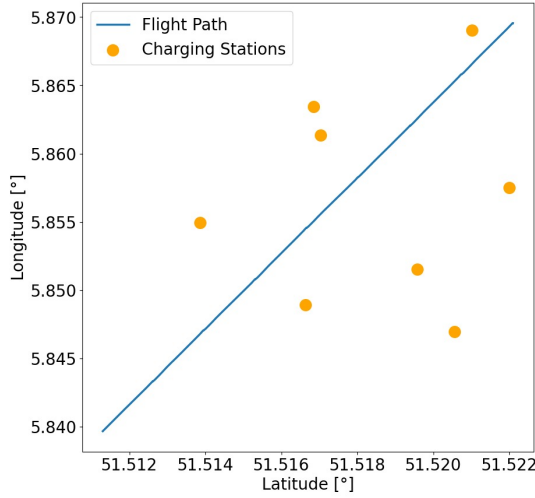


Fig. 19. Use Case # 2 analysis: a sketch of a UAV flight path with eight charging stations.

With OLO-RID in place, as the UAV discloses an obfuscated location, the system suggests the charging station closest to the reported obfuscated location. The best case is when the suggested charging station coincides with the ones that the system would have suggested if the actual UAV location was disclosed, as the extra distance to be travelled by the UAV because of the application of location obfuscation is 0 m. When this is not the case, the extra distance the UAV has to travel should be as small as possible. In the following, we investigate the utility of OLO-RID in this use case by evaluating the extra distance travelled by the UAV to reach the suggested charging station with different protocol configurations. We consider a UAV disclosing locations with average distance values of 25 m, 50 m, and 100 m, and a variable number of deployed charging stations, i.e., 2, 8, and 32, so to investigate the impact of a variable density of such charging stations on the utility of our solution. We summarize the results of our analysis in Tab. 5.

TABLE 5  
Extra distance travelled by the UAV in Use Case #2, with various configurations.

Avg. Distance [m]	No. of Charging Stations		
	2	8	32
Average Extra Distance [m]			
25	0.167	0.643	1.576
50	0.698	2.794	6.839
100	2.627	10.193	23.047

Increasing the average distance of the locations disclosed by the drone (i.e., increasing drone location privacy) leads to an increase in the average extra distance, i.e., the charging station suggested by the system is not optimal. At the same time, increasing the number of charging stations deployed by the system also increases the average extra distance, as there is more chance that another charging station is closer to the disclosed location than to the actual location. Asymptotically, if we consider an area completely filled with charging stations, there would always be a charging station coincidental with the UAV's disclosed location. Therefore,

the average extra distance asymptotically increases to match the average distance value. To provide further insights, we show in Figs. 20 and 21 the probability distribution of the extra distance travelled by the UAV considering the average distance of 100 m with 2 and 32 deployed charging stations, respectively. When the number of charging stations

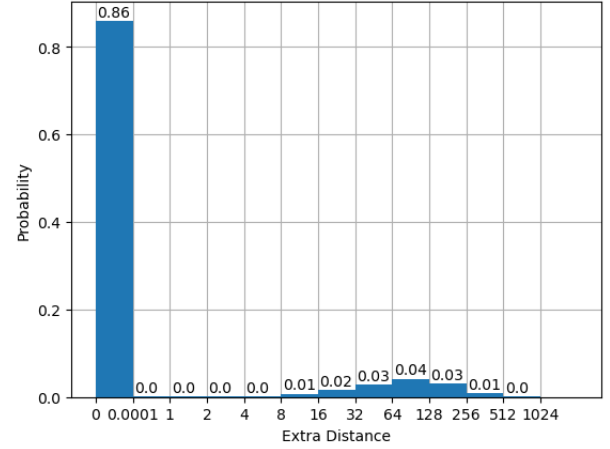


Fig. 20. Probability distribution of the average extra distance in Use Case #2, with an average distance of 100 m and 2 charging stations.

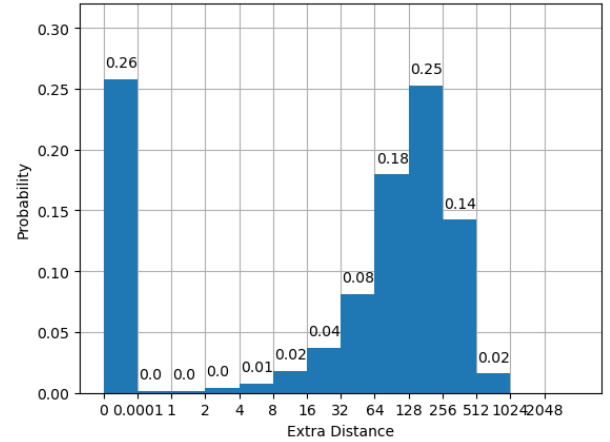


Fig. 21. Probability distribution of the average extra distance in Use Case #2, with average distance of 100 m and 32 charging stations.

(density) increases, the probability of picking a suboptimal charging station also increases. We also notice that, excluding the values for the extra distance 0 m, the remaining values tend to converge to a Gaussian distribution, with mean values coincidental with the average distance. Such a finding confirms our intuition that, asymptotically, the extra distance coincides with the average distance.

**Use Case 3: UAV as a service.** Consider Use Case #3 described in Sec. 3.3, and particularly, the scenario depicted in Fig. 22, where the blue marker depicts a user requesting a service and the yellow lines indicate the flight path of various UAVs providing services. Recall that the user finds the nearest UAV based on the location disclosed by such UAVs through RID messages. Without OLO-RID, the UAV suggested to the user would always be the one closest to



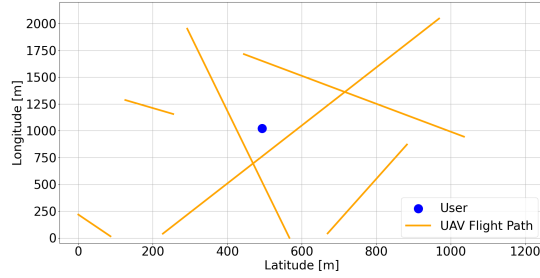


Fig. 22. Use Case #3 Analysis: (6) Flying UAVs providing a service and a user looking for service.

the user's location. With OLO-RID in place, although being farther than another UAV from the user, a given UAV might disclose a location closer to the user, being selected as the one providing the service to the user. In such cases, the wireless signals emitted by the user to the UAV propagate over an extra distance than the optimal case. In the following, we investigate the utility of OLO-RID in this use case by evaluating the extra distance the signal from the user has to travel to reach the suggested UAV based on the reported obfuscated location with different protocol configurations. We consider a variable number of deployed UAVs, i.e., 2, 6, and 10, and various values of average distance in the location disclosed by such UAVs, i.e., 25 m, 50 m, and 100 m. We summarize the results of our analysis in Tab. 6. We notice

TABLE 6  
Extra distance travelled by the signal in Use Case #3, with various configurations.

Avg. Distance [m]	No. of Service UAVs		
	2	6	10
Average Extra Distance [m]			
25	0.316	0.924	1.196
50	1.136	2.985	4.460
100	4.8432	11.764	16.636

that the results reported in Tab. 6 for Use Case #3 align with the ones in Tab. 5 for Use Case #2. Increasing the average distance, i.e., increasing drones' location privacy, leads to a higher extra distance, i.e., suboptimal performances of the location-based service. Similarly, increasing the number of UAVs increases the average extra distance, leading to suboptimal performances. We can apply the same reasoning as for Use Case #2 to reason about the asymptotic behavior of the extra distance in Use Case #3: assuming there is a UAV providing service on top of each possible location (i.e., an infinite number of UAVs), the average extra distance would match precisely the average distance. Finally, we notice a similarity between Use Case #2 and Use Case #3 also when analyzing the probability distribution of the extra distance for specific configurations, as shown in Figs. 23 and 24 considering an average distance of 100 m with 2 and 10 UAVs, respectively. When the UAVs providing services increase, the user's probability of picking the suboptimal UAV also increases. Excluding the values for the extra distance 0 m, the remaining values tend to converge to a Gaussian distribution, with mean values coincidental with the value of the average distance on the drone. This finding aligns

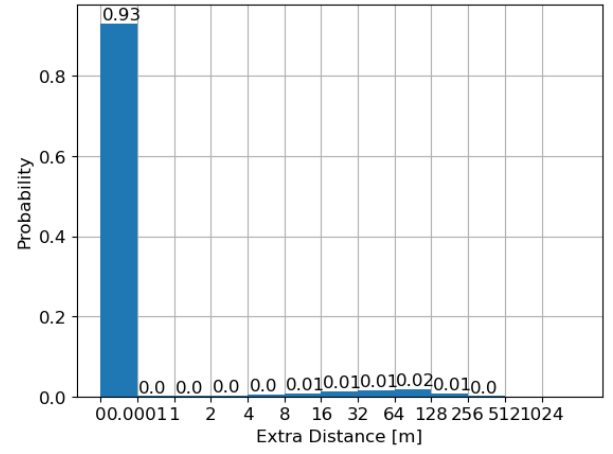


Fig. 23. Probability distribution of the average extra distance in Use Case #3 considering an average distance of 100 m and 2 service UAVs.

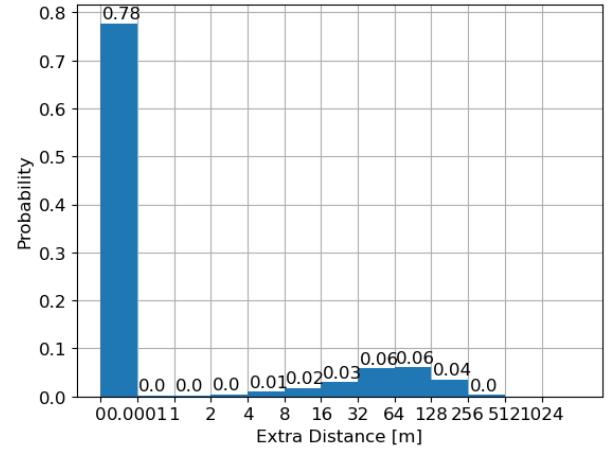


Fig. 24. Probability distribution of the average extra distance in Use Case #3 considering an average distance of 100 m and 10 service UAVs.

with our intuition that, asymptotically, the extra distance coincides with the average distance.

## 9 DISCUSSION

**Summary.** Through our extensive performance assessment (Sec. 8), we experimentally proved that OLO-RID allows to generate and deliver RID messages protecting the drones' location privacy within 0.16 s, i.e., below the threshold of 1 s set by the RID regulation [4]. The RAM consumption and communication overhead of our solution are also negligible, guaranteeing the potential smooth integration of our solution into running RID-compliant deployments.

**Energy Considerations.** As discussed in Sec. 8.2, a single RID message requires 0.149 mW and 0.216 mW of power for the ECs BN254 and BLS48556 on the RPI, respectively. Therefore, a single RID message requires 0.0140 mJ and 0.0147 mJ of energy for ECs BN254 and BLS48556, respectively. We can express such values in ampere-hours as  $Ah = E / (V \cdot 3600)$ , where  $Ah$  is the ampere-hours (Ah),  $E$  is the energy usage (J), and  $V$  is the voltage (V) of the battery of the UAV, e.g., 7.7 V for the DJI Mini 2 [37]. Therefore, a single

RID message secured through our solution requires from the UAV 0.000505  $\mu$ Ah and 0.000530  $\mu$ Ah for ECs BN254 and BLS48556, respectively. As the battery capacity of the DJI Mini 2 is 2250 mAh, OLO-RID consumes between 0.0224% and 0.0236% of the DJI Mini 2 total battery, confirming its limited energy overhead.

**Compliance to Requirements.** Here, we look back to the requirements defined in Sec.3.4 to evaluate the compliance of our solution. The requirement *R1, Location Obfuscation* is fulfilled by integrating and extending the solution in [9]. As per the requirement *R2, Trajectory Privacy*, as shown in Sec. 6, our system is as secure as the PIM method, so it offers trajectory privacy. Our solution does not require any Internet connection on the UAV, so it also fulfils the requirement *R3, No Persistent Internet Connection*. Internet connection might be required for some use cases discussed in Sec. 3.3, but the absence of such a connection does not prevent the drone from running OLO-RID. As per the requirement *R4, Maximum Message Generation Time.*, as shown in Sec. 8.2, the maximum time our solution takes to generate a RID message is always less than 0.16 seconds. Finally, as per the requirement *R5, Maximum Communication Overhead*, the modified RID message disclosed through OLO-RID is at most 227 bytes, below the MTU of WiFi of 2,304 bytes [21].

**RID Extension and Backward Compatibility.** To protect the UAVs' location privacy, OLO-RID extends the format of standard RID messages. Instead of delivering the actual UAV location, we deliver an *obfuscated location*, i.e., a location loosely correlated with the actual one, as described in Sec. 5. We also extend the standard RID message with *encrypted location reports*, containing the encryption of the actual UAV location through the public key of the USS. If necessary (see use case #1 in Sec. 3.3), the USS only can decrypt the UAV's actual location. Note that regular observers do not necessarily need to be updated to be able to decode the new cryptographic fields. General Public Observers can neglect those fields and only refer to the disclosed obfuscated location for the valid drone location. The only observers requiring software updates are the Public Safety Observers, likely connected to the USS for potential disclosure of the drones' actual location, if necessary. Therefore, our solution preserves backward compatibility with current deployments as much as possible while also enhancing the location privacy of RID-compliant drones.

**Utility Considerations.** Our experimental assessment (Sec. 8) provides insights into the trade-off between location privacy and utility to LBS. Consider drones obfuscating their location by an average distance of 100 meters. For the use case #1, CI operators using a small Warning Area achieve above 0.87 TP rate and only 0.14 of FP rate. For the use case #2, considering 10 deployed charging stations, the average extra distance travelled by the drone in an area of 1.5 km  $\times$  2.6 km  $\times$  40 m is only 23 m. Finally, for use case #3, considering the same area and 10 deployed service UAVs, the average extra distance travelled by the signal is only 16 m. Such results highlight that achieving higher location privacy than the standard RID regulation is possible while also guaranteeing meaningful utility of the disclosed location to LBSs. Recall that, whenever needed, relevant aviation authorities can decrypt the location report to recover the precise drone location.

## 10 CONCLUSION AND FUTURE WORK

In this paper, we proposed OLO-RID, a framework providing privacy-preserving location disclosure to RID-compliant drones. Through the integration of a state-of-the-art solution for correlated location disclosure and its extension for the drone scenario, OLO-RID allows drones to broadcast through RID messages obfuscated locations, protecting as much as possible trajectory privacy while dealing with processing, communication, memory, and energy constraints of the drones. OLO-RID also extends RID with encrypted location reports, allowing aviation authorities to obtain the actual drone location if necessary. We implemented two proofs-of-concept of our solution on a regular laptop and a RPI, and we experimentally show the viability of our solution for medium-end RID-compliant drones (0.16 s of RID message generation time and 0.0236% of energy for a DJI Mini 2). We also evaluate the utility of the disclosed location for three use cases involving drones usage, achieving a reasonable trade-off between drones location privacy and the quality of the provided service. Overall, our work demonstrates that we can achieve accountability for drone operations without entirely sacrificing privacy, paving the way for a practical real-world regulatory framework that considers all such requirements simultaneously.

## ACKNOWLEDGEMENTS

This work has been supported by the INTERSECT project, Grant No. NWA.1162.18.301, funded by the Netherlands Organisation for Scientific Research (NWO). The findings reported herein are solely responsibility of the authors.

## REFERENCES

- [1] H. Shakhatreh, A. Sawalmeh, A. Al-Fuqaha, et al., "Unmanned Aerial Vehicles (UAVs): A Survey on Civil Applications and Key Research Challenges," *IEEE Access*, vol. 7, pp. 48 572–48 634, 2019.
- [2] Statista, "Consumer drone unit shipments worldwide from 2020 to 2030," <https://www.statista.com/statistics/1234658/worldwide-consumer-drone-unit-shipments/#:~:text=The%20total%20number%20of%20consumer,unit%20shipments%20globally%20by%202030,2020>.
- [3] —, "Unmanned aircraft systems (UAS)/drones registered in the United States as of July 2023, by category," <https://www.statista.com/statistics/1221517/uas-drone-registrations-united-states/>, 2023.
- [4] FAA, "Remote identification of unmanned aircraft," 2021, accessed: Jan-15-2024. [Online]. Available: [https://www.faa.gov/sites/faa.gov/files/2021-08/RemoteID\\_Final\\_Rule.pdf](https://www.faa.gov/sites/faa.gov/files/2021-08/RemoteID_Final_Rule.pdf)
- [5] K. Belwafi, R. Alkadi, S. Alameri, et al., "Unmanned Aerial Vehicles' Remote Identification: A Tutorial and Survey," *IEEE Access*, vol. 10, pp. 87 577–87 601, 2022.
- [6] E. Wisse, P. Tedeschi, S. Sciancalepore, and R. D. Pietro, "A2RID -Anonymous Direct Authentication and Remote Identification of Commercial Drones," *IEEE Internet of Things J.*, pp. 1–1, 2023.
- [7] P. Tedeschi, S. Sciancalepore, and R. Di Pietro, "PPCA-Privacy-Preserving Collision Avoidance for Autonomous Unmanned Aerial Vehicles," *IEEE Transactions on Dependable and Secure Computing*, vol. 20, no. 2, pp. 1541–1558, 2022.
- [8] K. Chatzikokolakis, C. Palamidessi, and M. Stronati, "A predictive differentially-private mechanism for mobility traces," in *14th Int. Symp. on Privacy Enhancing Technologies*. Springer, 2014, pp. 21–41.
- [9] Y. Xiao and L. Xiong, "Protecting Locations with Differential Privacy under Temporal Correlations," in *Proc. of ACM Conf. on Computer and Communications Security*, 2015, p. 1298–1309.
- [10] A. Brighente, M. Conti, M. Schotsman, and S. Sciancalepore, "Open Source Code of OLO-RID," <https://github.com/MSchotsman/OLO-RID>, accessed: Jan-15-2024.

- [11] A. Brighente, M. Conti, and S. Sciancalepore, "Hide and Seek: Privacy-Preserving and FAA-Compliant Drones Location Tracing," in *Int. Conf. on Availability, Reliability and Security*, 2022.
- [12] "Drone remote id protocol (drip)," accessed: Jan-15-2024. [Online]. Available: <https://datatracker.ietf.org/wg/drip/about/>
- [13] S. W. Card, A. Wiethuechter, R. Moskowitz, and A. Gurtov, "Drone Remote Identification Protocol (DRIP) Requirements and Terminology," RFC 9153, Feb. 2022. [Online]. Available: <https://www.rfc-editor.org/info/rfc9153>
- [14] S. W. Card, A. Wiethuechter, R. Moskowitz, S. Zhao, and A. Gurtov, "Drone Remote Identification Protocol (DRIP) Architecture," RFC 9434, Jul. 2023. [Online]. Available: <https://www.rfc-editor.org/info/rfc9434>
- [15] D. R. L. Brown, "Sec 1: Elliptic curve cryptography," in *Standards for Efficient Cryptography*, vol. 2.0. Certicom Corp, 05 2009.
- [16] S. Sciancalepore and D. R. George, "Privacy-Preserving Trajectory Matching on Autonomous Unmanned Aerial Vehicles," in *Proceedings of the 38th Annual Computer Security Applications Conference*, 2022, pp. 1–12.
- [17] P. Tedeschi, S. Sciancalepore, and R. Di Pietro, "Lightweight Privacy-Preserving Proximity Discovery for Remotely-Controlled Drones," in *Proc. of Annual Computer Security Applications Conference*, 2023, pp. 178–189.
- [18] S. Sciancalepore, F. Kusters, N. K. Abdelhadi, and G. Oligeri, "Jamming Detection in Low-BER Mobile Indoor Scenarios via Deep Learning," *IEEE Internet of Things Journal*, 2023.
- [19] D. R. George, S. Sciancalepore, and N. Zannone, "Privacy-Preserving Multi-Party Access Control for Third-Party UAV Services," in *Proceedings of the 28th ACM Symposium on Access Control Models and Technologies*, 2023, pp. 19–30.
- [20] P. Tedeschi, S. Sciancalepore, and R. Di Pietro, "Modelling a Communication Channel under Jamming: Experimental Model and Applications," in *IEEE Intl Conf on Parallel & Distributed Processing with Applications, Big Data & Cloud Computing, Sustainable Computing & Communications, Social Computing & Networking*, 2021, pp. 1562–1573.
- [21] I. Standards, "IEEE Computer Society: "Part 11: Wireless LAN Medium Access Control (MAC) and Physical Layer (PHY) Specifications", IEEE Std 802.11™-2012, The Institute of Electrical and Electronics Engineers," 2012.
- [22] A. Svaigen, A. Boukerche, L. Ruiz, et al., "Design Guidelines of the Internet of Drones Location Privacy Protocols," *IEEE Internet of Things Mag.*, vol. 5, no. 2, pp. 175–180, 2022.
- [23] P. Tedeschi, S. Sciancalepore, and R. Di Pietro, "ARID: Anonymous Remote IDentification of Unmanned Aerial Vehicles," in *Annual Computer Security Applications Conference*, 2021, p. 207–218.
- [24] K. Sampigethaya and R. Poovendran, "Privacy of future air traffic management broadcasts," in *2009 IEEE/AIAA 28th Digital Avionics Systems Conference*, 2009, pp. 6.A.1–1–6.A.1–11.
- [25] A. R. Svaigen, A. Boukerche, L. B. Ruiz, and A. A. F. Loureiro, "A Topological Dummy-based Location Privacy Protection Mechanism for the Internet of Drones," in *ICC 2022 - IEEE International Conference on Communications*, 2022, pp. 1–6.
- [26] H. Jiang, J. Li, P. Zhao, et al., "Location privacy-preserving mechanisms in location-based services: A comprehensive survey," *ACM Comput. Surveys*, vol. 54, no. 1, pp. 1–36, 2021.
- [27] M. E. Andrés, N. E. Bordenabe, K. Chatzikokolakis, and C. Palamidessi, "Geo-indistinguishability: Differential privacy for location-based systems," in *Proc. of ACM conference on Computer & communications security*, 2013, pp. 901–914.
- [28] R. Mendes, M. Cunha, and J. Vilela, "Impact of Frequency of Location Reports on the Privacy Level of Geo-indistinguishability," *Proceedings on Privacy Enhancing Technologies*, vol. 2020, pp. 379–396, 04 2020.
- [29] J. Hua, F. Xu, and S. Zhong, "A geo-indistinguishable location perturbation mechanism for location-based services supporting frequent queries," *IEEE Transactions on Information Forensics and Security*, vol. 13, pp. 1155–1168, 2017.
- [30] W. Zhang, M. Li, R. Tandon, and H. Li, "Online location trace privacy: An information theoretic approach," *IEEE Transactions on Information Forensics and Security*, vol. 14, pp. 235–250, 2019.
- [31] X. Xiong, S. Liu, D. Li, J. Wang, and X. Niu, "Locally differentially private continuous location sharing with randomized response," *International Journal of Distributed Sensor Networks*, vol. 15, 2019.
- [32] Y. Xiao, L. Xiong, S. Zhang, and Y. Cao, "LocLok: Location Cloaking with Differential Privacy via Hidden Markov Model," *Proc. VLDB Endow.*, vol. 10, no. 12, p. 1901–1904, 08 2017. [Online]. Available: <https://doi.org/10.14778/3137765.3137804>
- [33] Y. Cao, Y. Xiao, L. Xiong, and L. Bai, "PriSTE: From location privacy to spatiotemporal event privacy," in *Int. Conf. on Data Engineering (ICDE)*. IEEE, 04 2019.
- [34] S. Enayati, D. Goeckel, A. Houmansadr, et al., "Location Privacy Protection for UAVs in Package Delivery and IoT Data Collection," *IEEE Internet of Things J.*, vol. 10, no. 23, pp. 20 586–20 601, 2023.
- [35] "Dji matrice 300 rtk," accessed: Jan-15-2024. [Online]. Available: <https://enterprise.dji.com/matrice-350-rtk?site=enterprise&from=nav>
- [36] "Raspberry pi 3 model b+," accessed: Jan-15-2024. [Online]. Available: <https://www.raspberrypi.com/products/raspberry-pi-3-model-b-plus/>
- [37] DJI, "Dji mini 2 specs," 2023, accessed: Jan-15-2024. [Online]. Available: <https://www.dji.com/nl/mini-2/specs>
- [38] "Miracl core," accessed: Jan-15-2024. [Online]. Available: <https://github.com/miracl/core>
- [39] P. Barreto and M. Naehrig, "Pairing-friendly elliptic curves of prime order," *Cryptology ePrint Archive*, Paper 2005/133, 2005, <https://eprint.iacr.org/2005/133>.
- [40] T. Kim and R. Barbulescu, "Extended tower number field sieve: A new complexity for the medium prime case," in *Annual international cryptology conference*. Springer, 2016, pp. 543–571.
- [41] M. Qu, "Sec 2: Recommended elliptic curve domain parameters," *Certicom Res., Tech. Rep. SEC2-Ver-0.6*, 1999.
- [42] Y. Kiyomura, A. Inoue, Y. Kawahara, et al., "Secure and efficient pairing at 256-bit security level," in *Int. Conf. on Applied Cryptography and Network Security*. Springer, 2017, pp. 59–79.
- [43] NATO, "Drone identification and tracking," 2021, accessed: Jan-15-2024. [Online]. Available: <https://www.kaggle.com/c/icmcis-drone-tracking/overview>